

Chapter 2

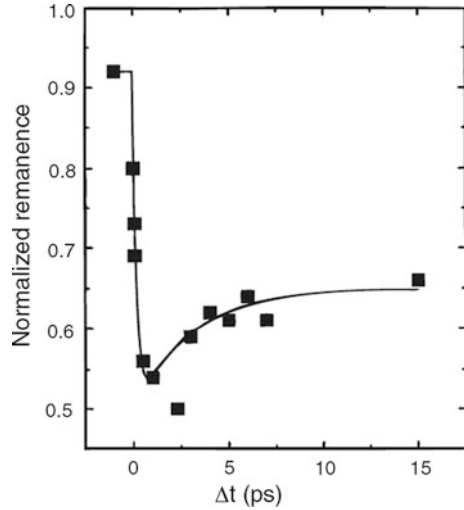
Spin Dynamics

As briefly mentioned in the introduction of Chap. 1, the spin dynamics has been a topic of intense research to address several intriguing fundamental physics issues. In this chapter, we describe various time scales involved with spin dynamics in detail. Earlier, external stimuli such as electrical excitation and optical excitation have been used to trigger the spin dynamics in ferromagnetic thin films, multilayers, and nanostructures [1–5]. Here, we introduce and summarize the theoretical and experimental studies pertaining to ultrafast optical manipulation of spins in ferromagnetic thin films and nanostructures. Theoretically, numerous interesting concepts are involved in understanding the spin dynamics, such as conservation of angular momentum and the associated coherent spin–photon interaction, role of magnetic anisotropies, many body exchange interaction, and relationship between fluctuation and dissipation. We present an overview of the different experimental and theoretical approaches and try to provide a comprehensive picture within which the effects of light on the net magnetization, magnetic anisotropy in the case of ferromagnetic thin films, and confined magnetic structures may be understood. It is also important to mention that understanding these mechanisms has a close relation to technological applications, in particular magnetic storage technology [3, 6]. The magnetization dynamics processes are potentially useful for writing and retrieving information in magnetic storage media in the fastest possible ways.

2.1 Phenomenological Description

As discussed in Chap. 1, when an ultrafast laser pulse excites a ferromagnetic material, the aftereffect of the interaction between the laser pulse and the ferromagnetic material becomes interesting. The technique of pump–probe measurements revolutionized experimental research in the spin-dynamics area. The advent of pulsed, femtosecond lasers in the late 1980s and early 1990s made possible to observe the phenomena where the effects are not solely given by the length of the

Fig. 2.1 Transient remanent longitudinal MOKE signal of a Ni(20 nm)/MgF₂(100 nm) film for 7 mJ cm⁻² pump fluence. The signal is normalized to the signal measured in the absence of pump beam. The line is a guide to the eye. *Reprinted with permission from Ref. [10]. Copyright 1996 by the American Physical Society*



pump and probe pulses. Experiments pioneering the laser excitation of ferromagnetic metals were conducted by Vaterlaus et al. on Gd [7, 8]. However, they worked with pump and probe pulses with pulse width of 10 ns and 60 ps, respectively. In 1991, Freeman et al. reported the picosecond TR-MOKE measurement of magnetization dynamics of magnetic thin film [9]. The first observation of magnetization dynamics on the sub-picosecond timescale was made by Beaurepaire et al. in 1996 [10] as reproduced in Fig. 2.1. Experimentally, it was found that a nickel thin film can be demagnetized in a sub-picosecond time scale after excitation with a sub-100 fs laser pulse. During the fs laser excitation, the photons are absorbed instantaneously via certain electronic states that have a direct influence on magnetic parameters, such as, the magnetocrystalline anisotropy. One of the main goals in the field of laser-induced spin dynamics is to develop and understand a microscopic model which can successfully describe ultrafast demagnetization which till date is the fastest event following laser pulse excitation of ferromagnetic thin films. We discuss below phenomenological models which can, in general, describe the experimental observations considering the energy flux and the transfer of the angular momentum between three reservoirs: electrons, spins, and the lattice. These models do not include certain microscopic mechanisms which give rise to ultrafast demagnetization, and hence, still this is one of the ongoing research topics in this field.

(a) Model Based on Rate Equations: Three-Temperature Model

The three-temperature model (3TM) is an extension of the two-temperature model (2TM) which is used for describing the experimental investigation of picosecond laser pulse excitation in normal metals. The 2TM was first developed for characterizing normal metals when it is subjected to laser-induced carrier dynamics [11]. Briefly, in 2TM, the electron and lattice are considered as heat reservoirs, and it is assumed that these are coupled to exchange energy between them. In order to

explain the magnetic system, Vaterlaus et al. [7] used the rate equation formulation by introducing the spin as one of the heat reservoirs. Within this model, the electron temperature T_e and lattice temperatures T_l characterize the electron and phonon distributions, whereas spin temperature T_s corresponds to spin distributions. In 3TM, it is assumed that the system consists of three thermalized reservoirs for exchanging energy, namely the electron, lattice, and spin systems at temperatures T_e , T_l , and T_s , respectively (Fig. 2.2). After the pump laser excitation of the magnetic thin films, within the first tens of fs, the experimentally observed non-equilibrium electron distribution cannot be described by a Fermi–Dirac distribution and thus no electron temperature can be derived. The absorbed energy creates hot electrons within the system, and during this transient hot electron regime, spin-dependent electron scattering modifies the spin population. This model was later invoked by Beaupaire et al. [10] to explain the experimental observation of ultrafast demagnetization as shown in Fig. 2.1. It is assumed that during this process, the spin dynamics associated with T_s is induced which is different from T_e to T_l . Finally, this results in ultrafast demagnetization of the ferromagnetic material. The temporal evolution of the system can be described by three coupled differential equations:

$$C_e(T_e) \frac{dT_e}{dt} = -g_{el}(T_e - T_l) - g_{es}(T_e - T_s) + P(t) \quad (2.1)$$

$$C_s(T_s) \frac{dT_s}{dt} = -g_{es}(T_s - T_e) - g_{sl}(T_s - T_l) \quad (2.2)$$

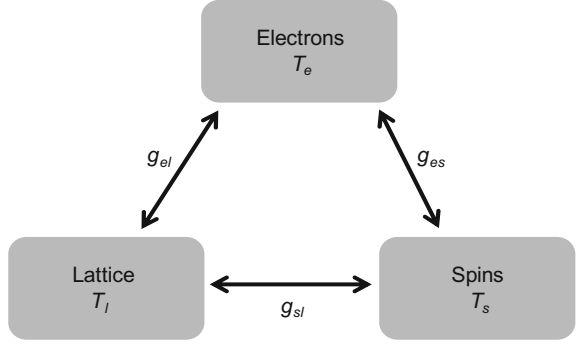
$$C_l(T_l) \frac{dT_l}{dt} = -g_{el}(T_l - T_e) - g_{sl}(T_l - T_s) \quad (2.3)$$

where C primarily refers to the specific heat, g refers to the coupling constant between the reservoirs, and the laser heating of the electron system is introduced using the term $P(t)$. More details of the symbols are listed below:

- C_e Electronic specific heat of the material concerned
- C_s Magnetic contribution to the specific heat
- C_l Lattice contribution to the specific heat
- g_{el} Electron–lattice interaction constant
- g_{sl} Spin–lattice interaction constant
- g_{es} Electron–spin interaction constant
- $P(t)$ Laser source term

The 3TM intuitively describes the energy equilibration processes during ultrafast demagnetization and the recovery of the magnetization back to equilibrium conditions. Using analytical solutions of the rate Eqs. (2.1) to (2.3), experimental demagnetization data has been fit by various groups. In order to simulate the energy equilibration processes between electrons, spins, and the lattice, input from experimental data, for example, the electron–lattice thermalization time from

Fig. 2.2 Schematic representing the electron, lattice, and spin reservoirs



reflectivity measurements is used. Readers may refer to interesting literatures for further details as we intend to provide an intuitive picture of the involved mechanisms without going into deep mathematical calculations [1]. It is important to mention here that study of ultrafast demagnetization has been performed in several materials where more than one magnetic constituents are present, for example, $\text{Ni}_{80}\text{Fe}_{20}$, CoPt, and Heusler alloys [12, 13]. In 2012, Mentink et al. developed a new model which explicitly includes the dynamics of multiple sublattices in a magnetic material of relativistic and exchange origin [14].

Though the 3TM can satisfactorily describe some experimental observations, but it is still a subject of intense debate due to some of its limitations. We further discuss other models that have been used to explain ultrafast demagnetization of ferromagnetic thin films which explicitly account for the transfer of spin angular momentum during ultrafast demagnetization by proposing photons and phonons as a reservoir for angular momentum.

(b) Model Based on Electron–Phonon Spin-Flip Scattering

In 2005, Koopmans et al. proposed that during ultrafast demagnetization, phonon-mediated spin-flip scattering is responsible for the spin angular momentum transfer to the lattice [15]. It was presumed that this spin-flip scattering is of the Elliot–Yafet (EY) [16, 17] type found in paramagnetic metals. It is further assumed that each electron–phonon scattering event can lead to a spin flip with a probability α_{EY} , which is material dependent. By extending the phenomenological 3TM with EY-like spin-flip channel, Koopmans named it as a microscopic three-temperature model (M3TM). Within this model, using ab initio density functional theory, the underlying spin-flip probability was calculated. A major limitation of M3TM was discussed by Carva et al. in 2011 [18], where it was shown the demagnetization rate in thermalized electron distributions as assumed under M3TM was significantly small. In another study in 2011, Essert et al. [19] surmised that the dynamical changes of the band structure play important role in the ultrafast demagnetization instead of electron–phonon spin-flip scattering as presumed in M3TM. Prior to these findings, in 2008, Carpena et al. [20] had proposed a spin-flip mechanism similar to the M3TM, but with magnons acting as the reservoir for spin angular

momentum, whereas, in 2009, Kraub et al. [21] had suggested a microscopic demagnetization mechanism based on electron–electron Coulomb scattering. Using these models, ultrafast demagnetization results of Ni and Co were reproduced by considering interband scattering processes which leads to a redistribution of electrons from majority to minority bands after the optical excitation of spin-polarized electrons.

(c) Model Based on Interaction Between Photons and Spins

Zhang and Hübner in 2000 [22] proposed a model for ultrafast demagnetization as a cooperative effect in the presence of both an external laser field and the internal spin–orbit coupling. It was concluded that in the absence of spin–orbit coupling, the laser field alone cannot change the magnetic moment on fs timescale; as well as without the laser field, the spin–orbit coupling can cause only few percent change in the magnetic moment. A major drawback of this model is the assumption that the pump laser photons serve as the source for the angular momentum needed to flip the spins in the ferromagnet. Under this condition, the mechanism of demagnetization should vary depending on the polarization of the pump laser beam if it is linearly or circularly polarized. Within a few years of the prediction by Zhang and Hübner, in 2007, Longa et al. [23] found that the magnetization dynamics remain unchanged by introducing any polarization-dependent changes in time-resolved magneto-optical Kerr effect (TR-MOKE) measurements. Furthermore, the model of Zhang and Hübner suggested that the ultrafast demagnetization has quasi-instantaneous nature and the observed time constant is given by the pump pulse length which remained controversial to be verified in the experiments. In 2009, Bigot et al. [24] proposed a similar microscopic mechanism in which a laser-field-induced time-dependent modification of the spin–orbit interaction was taken into account. Consideration of such effects leads to a coherent interaction between the pump photons and the spins. During this process, the transfer of angular momentum is necessary for the spin flips to occur.

(d) Model Based on Superdiffusive Spin Transport

A relatively advanced model to describe the origin of ultrafast demagnetization has been proposed by Battiato et al. in 2010 which takes into account the ‘superdiffusive spin transport’ [25]. Within this model, the reduction of magnetization is explained by spin-dependent transport of charge carriers out of a ferromagnetic layer instead of spin flips. It is assumed that due to pump laser irradiation of a ferromagnetic layer, electrons are excited from quasi-localized *d*-bands to more mobile *sp*-bands, and this process is spin conserving. Subsequently, electrons are transported superdiffusively out of the excited sample volume into the substrate. This phenomenon is referred as ‘superdiffusive’ due to the consideration of typical carrier transport which has ballistic character initially but converges to diffusive transport over longer time scale. Thus, for all timescales, either the ballistic or diffusive approximation fails to describe the carrier transport. It has been conjectured that the superdiffusive transport gives rise to ultrafast demagnetization

possibly due to the following mechanisms: (1) laser-excited electrons in *sp*-bands have high velocities, and (2) the lifetimes of the excited spin majority and minority electrons are different. As a result of the second point, the excited majority carriers in 3*d* ferromagnet are more mobile than the minority carriers which may lead to a deficit of majority carriers in the magnetic film and a transfer of magnetization away from the surface. For further details, readers may refer to detailed description in other relevant references [26, 27]. The next section describes the magnetization dynamics at various time-scales.

2.1.1 Magnetization Dynamics at Various Time Scales

A glimpse into the involved time scales in magnetism shows a very broad range varying from femtosecond to microsecond scale [1]. In the previous section, we described the ultrafast demagnetization which occurs during the first few hundreds of fs after laser irradiation of ferromagnetic thin films. It has been well established that the magnetization dynamics takes place on time scales that are usually longer than the time necessary in a ferromagnetic thin film to recover equilibrium between the carriers and the spin reservoir after the laser irradiation. The quantities such as saturation magnetization and effective anisotropy may be considered as time invariant over long time beyond fs regime. The precession of magnetization occurs within 10–100 ps and gets damped in sub-ns to tens of ns time [28]. Within similar time scales, two more phenomena, namely reversal of spins as used in magnetic recording (few ps—few hundreds of ps) and vortex core switching (few tens of ps—several ns), are known to happen. The slowest dynamics is the domain wall motion. The typical time scale of this process is few ns to few μ s. One of the motivations here is to understand the magnetization dynamics beyond the ultrafast demagnetization regime in ferromagnetic thin films and nanostructures with a particular focus on possibility of investigating magnetic damping. Earlier experimental studies showed that an ultrafast magnetic response can be used to trigger coherent precession of magnetization. In ferromagnetic materials, this study is considered as a first step toward an ultrafast and coherent optical control of magnetization which is significantly important for magnetic recording industry. Another interesting experimental study reported that the laser-induced demagnetization could be advantageous to trigger the magnetization precession in a ferromagnetic/antiferromagnetic exchange coupled system [29]. It was shown that the exchange bias between magnetic layers is modified by the ultrafast demagnetization to the point that the spin angular momentum is affected, leading to the precession of the magnetization on a time scale of a few hundreds of ps. The resulting process is coherent and decays within the characteristic dephasing time of the electronic levels. This discussed mechanism has been intensely used after this finding to optically induce the ferromagnetic resonance in the absence of any external radio frequency magnetic field.

2.1.2 *Optically Induced Ultrafast Spin Dynamics*

The unique feature of optically induced ultrafast spin dynamics is it allows accessing the dynamics over fs to ns time scale. Intense research on experimental and theoretical fronts was pursued after the seminal work of observation of ultrafast demagnetization by Beaurepaire et al. in 1996 [10]. Koopmans et al., in 2000, debated over the origin of observed magneto-optical signal obtained during magnetization dynamics measurement in Ni [30]. The main concern of these authors was whether the experimental signal observed has purely magnetic origin or it also contains optical contributions. In their study, the authors explicitly measured the time-resolved Kerr ellipticity and rotation, as well as its temperature and magnetic field dependence in epitaxially grown (111)- and (001)-oriented Cu/Ni/Cu wedge-shaped thin films with Ni thickness varying from 0 to 15 nm. Their main finding was that in the first hundreds of fs, the response is dominated by state-filling effects, whereas the actual demagnetization occurs in approximately 0.5–1 ps, and in the sub-ns time scale regime, the spins precess in the anisotropy field. Within two years of this study, in 2002, van Kampen et al. [28] showed a novel all-optical method of excitation and detection of spin waves which is considered to be a major breakthrough in generalizing the laser-induced magnetization dynamics in ferromagnetic thin films. Despite of the fact that the above-mentioned phenomenon is described in the existing literatures, for the sake of completeness of the discussion, here, we emphasize the damping aspect of the experimental result (cf. Fig. 2.3). In this study, a polycrystalline Ni thin film deposited on silicon substrate with a canted equilibrium orientation of magnetization in an external applied field was investigated using a pump-probe-based TR-MOKE magnetometer. The schematic of the experimental setup is shown in Fig. 2.3a with an arrangement of focusing the pump and probe laser beams on the sample along with the provision of external magnetic field application. When the pump pulse hits the Ni film, a sharp decrease in the perpendicular component of magnetization M_z is observed. Primarily, the change in magnitude of the (temperature-dependent) magnetization is responsible for such decrease. It is followed by a subsequent recovery of M_z on a time scale of a few ps which is due to rapid heat diffusion into the substrate. Remarkably, over few hundreds of ps post-thermal equilibrium, a secondary response appears in the TR-MOKE signal as a persistent oscillation as shown in Fig. 2.3b. A delicate balance between the external field and the net anisotropy field of the film determines the canting angle. The transient heating of the Ni film due to pump pulse also results in the change in anisotropy of the film. This causes a change of the equilibrium orientation of M from θ_c to θ_c' as indicated in Fig. 2.3c (IIa), triggering an initial precession of the magnetization around its new equilibrium orientation as schematically represented in (IIb). For the case of metallic films, the original equilibrium angle is restored after around 10 ps of removal of excess heat by heat diffusion into the thin film. It is interesting to note here that up to this point, the magnetization is still not in equilibrium due to its initial displacement. Thus, the magnetization continues to precess for few hundreds of ps as shown in scheme (III).

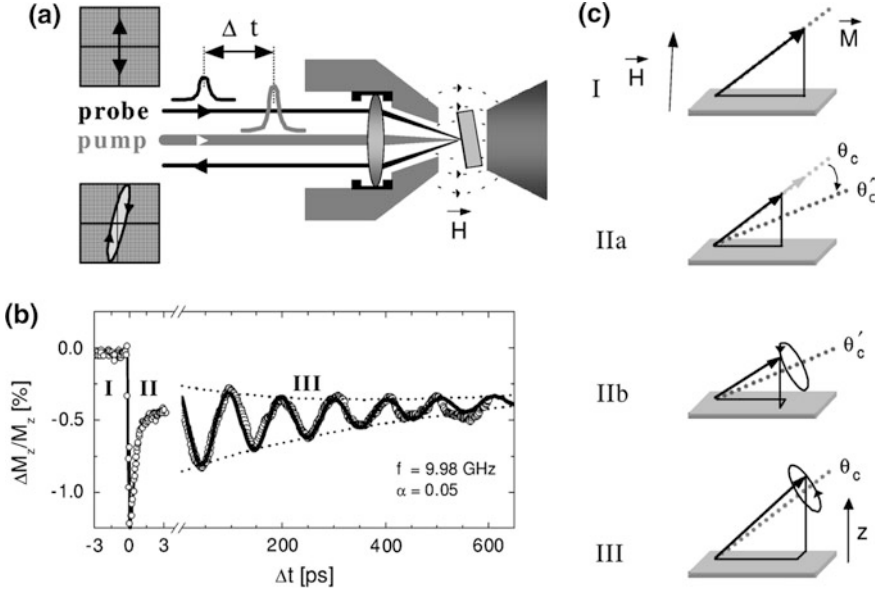


Fig. 2.3 Schematic pump-probe setup. **a** The magnetization is measured by the polarization state of the reflected probe pulse. **b** Typical measurement on a 7 nm Ni film (open circles: data; thick line: fit) displaying the perpendicular component of the magnetization, M_z , as a function of delay time Δt . The different stages are indicated by numbers. **c** The stages of the excitation process: (I) $\Delta t < 0$, the magnetization \vec{M} points in equilibrium direction (dotted line), (IIa) $\Delta t = 0$, the magnitude of \vec{M} and the anisotropy change due to heating, thereby altering the equilibrium orientation, (IIb) $0 < \Delta t < 10$ ps, \vec{M} starts to precess around its new equilibrium, (III) $\Delta t > 10$ ps, heat has diffused away, the magnitude of \vec{M} and anisotropy are restored, but the precession continues because of the initial displacement of \vec{M} . *Reprinted with permission from Ref. [28]. Copyright 2002 by the American Physical Society*

However, in a real system, energetically it is not favored for the magnetization to precess for infinitely long duration. Importantly, the effective damping (α_{eff}) governs the magnetization dynamics till the time the magnetization relaxation occurs. Furthermore, in this study, it was found that the laser-induced spin precession in single magnetic layer has equivalence with the frequency as observed in a ‘conventional ferromagnetic resonance (FMR)’ experiment, and the damping constant of the Ni film estimated using TR-MOKE and FMR technique is consistent. This led to the establishment of a sensitive optical excitation and detection tool which may be used to study coherent magnetization dynamics including important aspects of damping phenomena in ferromagnetic thin films. An important question which kept puzzling the research community working in this field was if optical excitation and detection-based technique can be implemented for investigating the

magnetization dynamics, in particular, for estimating the effective damping coefficient ' α_{eff} ', in magnetic nanostructures.

In 2006, Barman et al. [4] developed the technique of Cavity Enhanced-TR-MOKE (more details of this technique will be discussed in Chap. 4 of this book) to investigate ultrafast magnetization dynamics in ferromagnetic nano-elements. Later in 2007 [31], the authors reported a size-dependent effective damping (α_{eff}) of nickel nanomagnets (cylindrical nickel dots with constant height of 150 nm and with varying diameter D from 5 μm down to 125 nm) extracted directly from the time-resolved Kerr rotation. The dots were coated with 70-nm-thick SiN layer to have a fivefold increase in the Kerr rotation due to cavity enhancement. Traces of the TR-MOKE data as observed in their study are reproduced in Fig. 2.4a. High-pass fast Fourier transform filtering of the experimental time-resolved data was performed to eliminate any low-frequency background. The filtered time-resolved data was shown to possess a single uniform precession frequency, and these were fitted through a least square fitting routine with a damped sine function of the form

$$M(t) = M(0)e^{-t/\tau}\sin(\omega t - \phi) \quad (2.4)$$

where τ is the decay time of the precession defined as $\tau = 1/\omega\alpha_{\text{eff}}$, ω is the angular frequency of the uniform precession mode given by $\omega = \gamma H_{\text{eff}}$, ϕ is the initial phase of oscillation, γ is the gyromagnetic ratio, and H_{eff} is the effective magnetic field. Briefly, in this study, large qualitative and quantitative differences in between the microscale and nanoscale magnetic nanodots were observed (Fig. 2.4b). It was found that for nanomagnet of diameter 2 μm , α_{eff} reduces sharply. Furthermore, a slow decrease in α_{eff} down to 500 nm was observed where it attains a value 0.04, comparable to the reported damping coefficient 0.05 of continuous Ni thin film measured by all-optical method. In Fig. 2.4c, a representative time-resolved data from a magnetic dot of 400 nm diameter at varying external bias field is shown. It was inferred from these data that the α_{eff} almost remains invariant with respect to external bias field. Overall, they reported that for the magnetic elements with $D > 2 \mu\text{m}$ a strong bias field dependence of α_{eff} was observed, while for those with $D < 1 \mu\text{m}$, no bias field dependence was observed. For magnetic elements with intermediate D , weak bias field dependence was observed. The above observations established that the all-optical excitation and detection are well suited for investigating the magnetization dynamics, including damping behavior in magnetic nanostructures. It is worth mentioning here that the research on laser-induced magnetization dynamics, in particular, the ultrafast demagnetization, different relaxation mechanisms, and investigation of precession frequency and effective damping behavior have grown significantly over the last decade and to cover all details of those is beyond the scope of this book.

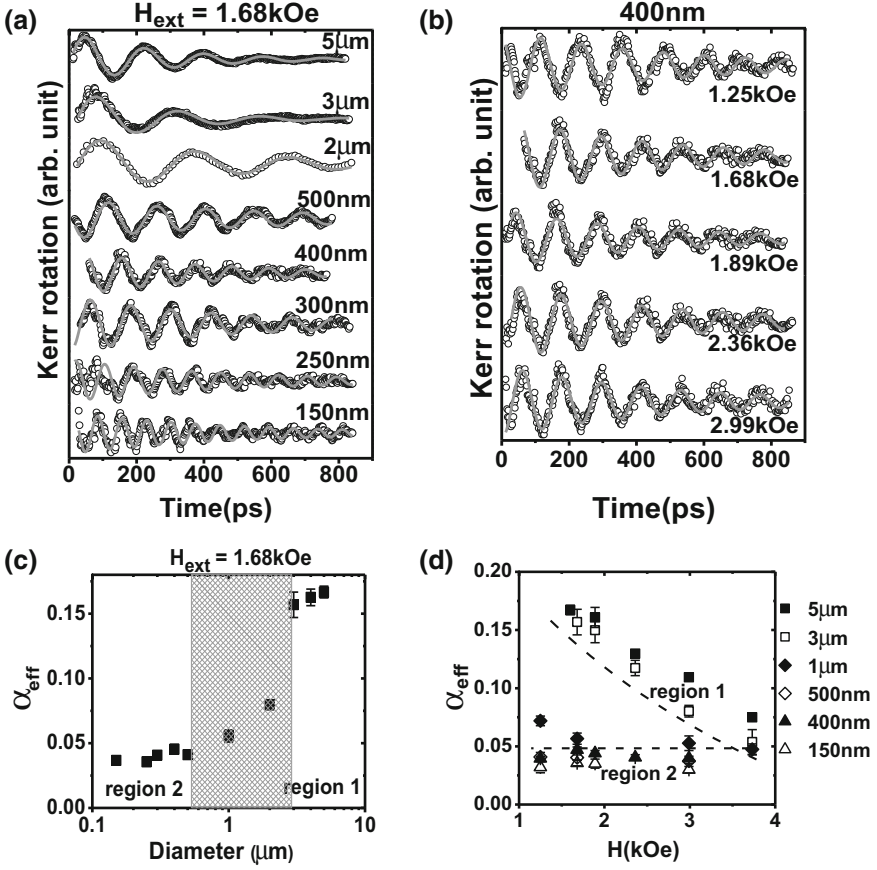


Fig. 2.4 **a** Experimental (*open circles*) and fitted (*gray lines*) time-resolved data from magnetic dots of varying diameter at an external bias field = 1.68 kOe. **b** The extracted effective damping coefficient α_{eff} as a function of magnet diameter. The hatched rectangle shows the transition region from a high to low α_{eff} . **c** Experimental (*open circles*) and simulated (*gray lines*) time-resolved data from a magnetic dot of 400 nm diameter at varying external bias fields. **d** The extracted α_{eff} for magnets with varying diameter as a function of the external bias field. A high-pass FFT filtering was applied to the experimental time-resolved data for fitting with a single damped sine function. Reprinted with permission from Ref. [31]. Copyright 2007 by the American Institute of Physics

2.1.3 Landau–Lifshitz–Gilbert (LLG) Equation

Following quantum mechanics, equation of motion for the dynamics of single spin can be derived, and it is known as Landau–Lifshitz (LL) [32] equation mentioned as below

$$\frac{d}{dt} \langle S \rangle = \frac{g\mu_B}{\hbar} \langle S \times B \rangle \quad (2.5)$$

where S denotes spin and B the magnetic field, and the multiplicative term corresponds to the gyromagnetic ratio $\gamma = g\mu_B/\hbar$. In the macroscopic model, the magnetization vector is defined by uniform distribution of spin in the sample, and it is expressed as below:

$$\mathbf{M} = -\frac{g\mu_B}{\hbar} \langle S \rangle \quad (2.6)$$

Therefore, equation of motion of magnetization in presence of external magnetic field is given by

$$\frac{d\mathbf{M}}{dt} = -\frac{g\mu_B}{\hbar} \langle \mathbf{M} \times \mathbf{H} \rangle \quad (2.7)$$

Equation (2.7) is known as Landau–Lifshitz (LL) equation, and this is generalized by using H_{eff} in place of H . The Landau–Lifshitz model considers that the total magnetic moment is related to the total angular momentum which experiences the net torque resulting in a precessional motion. It thus implies that the tip of the magnetization vector precesses around the effective magnetic field in a circular orbit as shown in Fig. 2.5a for infinite duration with angular frequency $\omega = \gamma H_{\text{eff}}$. However, in all practical situations, the precession amplitude of magnetization decreases with time, and the tip of the magnetization vector follows a spiral path as shown in Fig. 2.5b. Thus, in order to describe real magnetization dynamics, a damping term needs to be included in the LL equation.

For practical systems, Gilbert [33, 34] proposed a phenomenological term used to describe the damping of the magnetization precession. Depending on the time derivative of the magnetization, Gilbert modeled a ‘viscous’ damping by

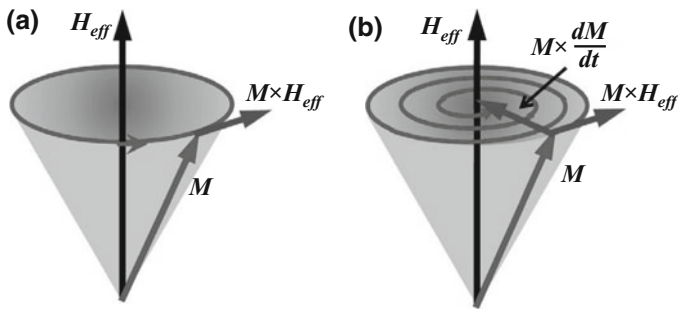


Fig. 2.5 Precession of magnetization about the applied bias field **a** without damping and **b** with damping

considering a phenomenological dissipation term. The precessional dynamics is described by Landau–Lifshitz–Gilbert (LLG) Eq. (2.8)

$$\frac{d\vec{M}}{dt} = -\gamma(\vec{M} \times \vec{H}_{\text{eff}}) + \frac{\alpha}{M} \left(\vec{M} \times \frac{d\vec{M}}{dt} \right) \quad (2.8)$$

where α the dimensionless Gilbert damping and γ the gyromagnetic ratio. The effective magnetic field

$$H_{\text{eff}} = H_{\text{a}} + H_{\text{dem}} + H_{\text{ext}} + H_{\text{exc}}$$

is composed of anisotropy fields (H_{a}), the demagnetizing field (H_{dem}), external applied magnetic field (H_{ext}), and exchange field (H_{exc}). Importantly, similar to the LL model, the magnitude of the magnetization is conserved in the LLG equation as well. To reiterate, the Gilbert damping term was specifically introduced to replicate the experimental observation in the best conceivable manner. The LLG equation has been used to study the magnetization dynamics in various magnetic systems. If the magnetic system is sufficiently small, then the magnetization may be assumed to remain uniform during the dynamics, and anisotropy field, demagnetizing field, and the applied external field contribute to the effective field. For larger samples and in the case of inhomogeneous dynamics, the magnetic moment becomes a function of spatial coordinates. The effective magnetic field in this case also acquires a contribution from the exchange interaction. In such situation, non-homogeneous elementary excitations of the magnetic medium may exist, first proposed by Felix Bloch in 1930 [35]. These excitations are called spin waves and involve many lattice sites. More details on these aspects can be found in existing literatures [36]. Commonly, it has been thought that intrinsic Gilbert damping had its origin in spin–orbit coupling because this mechanism does not conserve spin, but it has never been derived from a coherent framework. For ferromagnetic thin films and nanostructures, the non-local spin relaxation processes and disorder broadening couple to the spin dynamics and leads to enhanced Gilbert damping. One of the well accepted ways of confirming the form of damping is to understand the ferromagnetic resonance spectral linewidth. The damping constant is often reformulated in terms of a relaxation time, and the dominant relaxation processes are invoked to calculate it. In Chap. 3 of this book, we will describe the damping in more detail.

References

1. Kirilyuk A, Kimel AV, Rasing T (2010) Ultrafast optical manipulation of magnetic order. *Rev Mod Phys* 82(3):2731–2784. doi:[10.1103/RevModPhys.82.2731](https://doi.org/10.1103/RevModPhys.82.2731)
2. Tserkovnyak Y, Brataas A, Bauer GEW, Halperin BI (2005) Nonlocal magnetization dynamics in ferromagnetic heterostructures. *Rev Mod Phys* 77(4):1375–1421. doi:[10.1103/RevModPhys.77.1375](https://doi.org/10.1103/RevModPhys.77.1375)

3. Hoffmann A, Bader SD (2015) Opportunities at the Frontiers of spintronics. *Phys Rev Appl* 4 (4):047001. doi:[10.1103/PhysRevApplied.4.047001](https://doi.org/10.1103/PhysRevApplied.4.047001)
4. Barman A, Wang S, Maas JD, Hawkins AR, Kwon S, Liddle A, Bokor J, Schmidt H (2006) Magneto-optical observation of picosecond dynamics of single nanomagnets. *Nano Lett* 6 (12):2939–2944. doi:[10.1021/nl0623457](https://doi.org/10.1021/nl0623457)
5. Liu L, Pai C-F, Li Y, Tseng HW, Ralph DC, Buhrman RA (2012) Spin-torque switching with the giant spin Hall effect of tantalum. *Science* 336(6081):555–558. doi:[10.1126/science.1218197](https://doi.org/10.1126/science.1218197)
6. Bader SD (2006) Opportunities in nanomagnetism. *Rev Mod Phys* 78(1):1–15. doi:[10.1103/RevModPhys.78.1](https://doi.org/10.1103/RevModPhys.78.1)
7. Vaterlaus A, Beutler T, Meier F (1991) Spin-lattice relaxation time of ferromagnetic gadolinium determined with time-resolved spin-polarized photoemission. *Phys Rev Lett* 67 (23):3314–3317. doi:[10.1103/PhysRevLett.67.3314](https://doi.org/10.1103/PhysRevLett.67.3314)
8. Vaterlaus A, Beutler T, Guarisco D, Lutz M, Meier F (1992) Spin-lattice relaxation in ferromagnets studied by time-resolved spin-polarized photoemission. *Phys Rev B* 46 (9):5280–5286. doi:[10.1103/PhysRevB.46.5280](https://doi.org/10.1103/PhysRevB.46.5280)
9. Freeman MR, Ruf RR, Gambino RJ (1991) Picosecond pulsed magnetic fields for studies of ultrafast magnetic phenomena. *IEEE Trans Magn* 27(6):4840–4842. doi:[10.1109/20.278964](https://doi.org/10.1109/20.278964)
10. Beaurepaire E, Merle JC, Daunois A, Bigot JY (1996) Ultrafast spin dynamics in ferromagnetic nickel. *Phys Rev Lett* 76(22):4250–4253. doi:[10.1103/PhysRevLett.76.4250](https://doi.org/10.1103/PhysRevLett.76.4250)
11. Kaganov MI, Lifshitz IM, Tanatarov LV (1957) Relaxation between electrons and the crystalline lattice. *J Exp Theor Phys* 4(2):173
12. Guidoni L, Beaurepaire E, Bigot J-Y (2002) Magneto-optics in the ultrafast regime: thermalization of spin populations in ferromagnetic films. *Phys Rev Lett* 89(1):017401. doi:[10.1103/PhysRevLett.89.017401](https://doi.org/10.1103/PhysRevLett.89.017401)
13. Mann A, Walowski J, Münzenberg M, Maat S, Carey MJ, Childress JR, Mewes C, Ebke D, Drewello V, Reiss G, Thomas A (2012) Insights into ultrafast demagnetization in pseudogap half-metals. *Phys Rev X* 2(4):041008. doi:[10.1103/PhysRevX.2.041008](https://doi.org/10.1103/PhysRevX.2.041008)
14. Mentink JH, Hellsvik J, Afanasiev DV, Ivanov BA, Kirilyuk A, Kimel AV, Eriksson O, Katsnelson MI, Rasing T (2012) Ultrafast spin dynamics in multisublattice magnets. *Phys Rev Lett* 108(5):057202. doi:[10.1103/PhysRevLett.108.057202](https://doi.org/10.1103/PhysRevLett.108.057202)
15. Koopmans B, Ruigrok JJM, Longa FD, de Jonge WJM (2005) Unifying ultrafast magnetization dynamics. *Phys Rev Lett* 95(26):267207. doi:[10.1103/PhysRevLett.95.267207](https://doi.org/10.1103/PhysRevLett.95.267207)
16. Elliott RJ (1954) Theory of the effect of spin-orbit coupling on magnetic resonance in some semiconductors. *Phys Rev* 96(2):266–279. doi:[10.1103/PhysRev.96.266](https://doi.org/10.1103/PhysRev.96.266)
17. Yafet Y (1963) Solid state physics vol. 14. Academic Press
18. Carva K, Battiato M, Oppeneer PM (2011) Ab initio investigation of the Elliott-Yafet electron-phonon mechanism in laser-induced ultrafast demagnetization. *Phys Rev Lett* 107 (20):207201. doi:[10.1103/PhysRevLett.107.207201](https://doi.org/10.1103/PhysRevLett.107.207201)
19. Essert S, Schneider HC (2011) Electron-phonon scattering dynamics in ferromagnetic metals and their influence on ultrafast demagnetization processes. *Phys Rev B* 84(22):224405. doi:[10.1103/PhysRevB.84.224405](https://doi.org/10.1103/PhysRevB.84.224405)
20. Carpenne E, Mancini E, Dallera C, Brenna M, Puppini E, De Silvestri S (2008) Dynamics of electron-magnon interaction and ultrafast demagnetization in thin iron films. *Phys Rev B* 78 (17):174422. doi:[10.1103/PhysRevB.78.174422](https://doi.org/10.1103/PhysRevB.78.174422)
21. Krauß M, Roth T, Alebrand S, Steil D, Cinchetti M, Aeschlimann M, Schneider HC (2009) Ultrafast demagnetization of ferromagnetic transition metals: the role of the Coulomb interaction. *Phys Rev B* 80(18):180407. doi:[10.1103/PhysRevB.80.180407](https://doi.org/10.1103/PhysRevB.80.180407)
22. Zhang GP, Hübner W (2000) Laser-induced ultrafast demagnetization in ferromagnetic metals. *Phys Rev Lett* 85(14):3025–3028. doi:[10.1103/PhysRevLett.85.3025](https://doi.org/10.1103/PhysRevLett.85.3025)
23. Dalla Longa F, Kohlhepp JT, de Jonge WJM, Koopmans B (2007) Influence of photon angular momentum on ultrafast demagnetization in nickel. *Phys Rev B* 75(22). doi:[10.1103/PhysRevB.75.224431](https://doi.org/10.1103/PhysRevB.75.224431)

24. Bigot JY, Vomir M, Beaupaire E (2009) Coherent ultrafast magnetism induced by femtosecond laser pulses. *Nat Phys* 5(7):515–520. doi:[10.1038/nphys1285](https://doi.org/10.1038/nphys1285)
25. Battiato M, Carva K, Oppeneer PM (2010) Superdiffusive spin transport as a mechanism of ultrafast demagnetization. *Phys Rev Lett* 105(2):027203. doi:[10.1103/PhysRevLett.105.027203](https://doi.org/10.1103/PhysRevLett.105.027203)
26. Carva K, Battiato M, Oppeneer PM (2011) Is the controversy over femtosecond magneto-optics really solved? *Nat Phys* 7(9):665. doi:[10.1038/nphys2067](https://doi.org/10.1038/nphys2067)
27. Eschenlohr A, Battiato M, Maldonado R, Pontius N, Kachel T, Holldack K, Mitzner R, Fohlisch A, Oppeneer PM, Stamm C (2013) Ultrafast spin transport as key to femtosecond demagnetization. *Nat Mater* 12(4):332–336. doi:[10.1038/nmat3546](https://doi.org/10.1038/nmat3546)
28. van Kampen M, Jozsa C, Kohlhepp JT, LeClair P, Lagae L, de Jonge WJM, Koopmans B (2002) All-optical probe of coherent spin waves. *Phys Rev Lett* 88(22):227201. doi:[10.1103/PhysRevLett.88.227201](https://doi.org/10.1103/PhysRevLett.88.227201)
29. Ju G, Nurmikko AV, Farrow RFC, Marks RF, Carey MJ, Gurney BA (1999) Ultrafast time resolved photoinduced magnetization rotation in a ferromagnetic/antiferromagnetic exchange coupled system. *Phys Rev Lett* 82(18):3705–3708. doi:[10.1103/PhysRevLett.82.3705](https://doi.org/10.1103/PhysRevLett.82.3705)
30. Koopmans B, van Kampen M, Kohlhepp JT, de Jonge WJM (2000) Ultrafast magneto-optics in nickel: magnetism or optics? *Phys Rev Lett* 85(4):844–847. doi:[10.1103/PhysRevLett.85.844](https://doi.org/10.1103/PhysRevLett.85.844)
31. Barman A, Wang S, Maas J, Hawkins AR, Kwon S, Bokor J, Liddle A, Schmidt H (2007) Size dependent damping in picosecond dynamics of single nanomagnets. *Appl Phys Lett* 90:202504. doi:[10.1063/1.2740588](https://doi.org/10.1063/1.2740588)
32. Landau L, Lifshitz E (1935) On the theory of the dispersion of magnetic permeability in ferromagnetic bodies. *Physikalische Zeitschrift der Sowjetunion* 8(153):101–114
33. Gilbert TL (2004) A phenomenological theory of damping in ferromagnetic materials. *IEEE Trans Magn* 40(6):3443–3449. doi:[10.1109/tmag.2004.836740](https://doi.org/10.1109/tmag.2004.836740)
34. Gilbert TL (1955) A Lagrangian formulation of the gyromagnetic equation of the magnetic field. *Phys Rev* 100:1243
35. Bloch F (1930) Zur Theorie des Ferromagnetismus. *Zeitschrift für Physik* 61:206
36. Demokritov SO, Hillebrands B, Slavin AN (2001) Brillouin light scattering studies of confined spin waves: linear and nonlinear confinement. *Phys Rep* 348(6):441–489. doi:[10.1016/S0370-1573\(00\)00116-2](https://doi.org/10.1016/S0370-1573(00)00116-2)

Spin Dynamics and Damping in Ferromagnetic Thin
Films and Nanostructures

Barman, A.; Sinha, J.

2018, XI, 156 p. 53 illus., 35 illus. in color., Hardcover

ISBN: 978-3-319-66295-4